Acta Geodyn. Geomater., Vol. 19, No. 3 (207), 255–270, 2022
DOI: 10.13168/AGG.2022.0011

journal homepage: https://www.irsm.cas.cz/acta

ORIGINAL PAPER

MULTI-GNSS POSITIONING FOR LANDSLIDE MONITORING: A CASE STUDY AT THE RECICA LANDSLIDE

Weiguo LI [1], Michal KAČMAŘÍK [1] * and Pavel POSPÍŠIL [2]

[1] *Department of Geoinformatics, VŠB-Technical University of Ostrava, 70800 Ostrava, Czech Republic*
[2] *Department of Geotechnics and Underground Engineering, VŠB-Technical University of Ostrava, 70800 Ostrava, Czech Republic*

**Corresponding author's e-mail:* michal.kacmarik@vsb.cz

ARTICLE INFO

Article history:
Received 13 May 2022
Accepted 25 July 2022
Available online 6 August 2022

Keywords:
GNSS
Multi-GNSS
Landslide
PPP
RTKLIB

ABSTRACT

Global Navigation Satellite System (GNSS) positioning has characteristics of simple operation, high efficiency and high precision technique for landslide surface monitoring. In recent years, finalization of modern GNSS systems Galileo and BeiDou has brought a possibility of multi-GNSS positioning. The paper focuses on evaluation of possible benefits of multi-GNSS constellations in landslide monitoring. While simulating observational conditions of selected Recica landslide in the Czech Republic, one-month data from well-established permanent GNSS reference stations were processed. Besides various constellation combinations, differential and Precise Point Positioning techniques, observation data lengths and observation sampling intervals were evaluated. Based on the results, using a combination of GPS and GLONASS, or GPS, GLONASS and Galileo systems can be recommended, together with a static differential technique and observation periods for data collection exceeding eight hours. In the last step, data from GNSS repetitive campaigns realized at the Recica landslide during two years were processed with optimal setup and obtained displacement results were compared to standard geotechnical measurements.

1. INTRODUCTION

Landslides belong to natural hazards which can cause significant economic and life losses (Vega et al., 2019). Those which are representing a potential threat are usually actively monitored. Selection of suitable monitoring methods and instruments generally depend on landslide type, its geological characteristics, surrounding environment and present trigger factors (González-Díez et al., 1999; Castagnetti et al.; 2013, Soto et al., 2017; Su et al., 2017; Pecoraro et al., 2019). For landslide surface monitoring, Global Navigation Satellite System (GNSS) has become one of the most useful technologies due to its relatively simple operation, high efficiency and high precision (Gili et al., 2000; Malet et al., 2002; Calcaterra et al., 2012; Devoti et al., 2015).

With respect to local topography, GNSS receivers located at landslides can have somehow limited view over the sky which can lead to a lower number of visible satellites and in overall to poorer observation conditions. Together with a potential of multipath effects caused by changing vegetation or other sources around the receiver (Han et al., 2018), all these effects can lead to a decrease of positioning accuracy.

With a modernization of legacy GPS and GLONASS systems, as well as with a finalization of the new European Galileo and Chinese BeiDou systems, about 120 navigation satellites for GNSS users around the world are available presently (Li et al., 2022). Higher number of satellites is expected to lead to a higher robustness of GNSS solutions and under some conditions also to a higher accuracy and precision of positioning. Usage of multi-GNSS constellations has therefore become an important research topic in recent years (Li et al., 2015; Montenbruck et al., 2017; Pan et al., 2017; Pan et al., 2019; Li et al., 2020; Li and Kačmařík, 2021; Paziewski et al., 2021). However, most of the studies use data from the International GNSS Service (IGS) Multi-GNSS Experiment (MGEX, https://igs.org/mgex/) or from other permanent multi-GNSS stations with optimal observational environments. Their processing strategies are typically utilizing daily datasets with 30 s observation sampling interval.

In the landslide mapping and monitoring, majority of works in recent years were still based on legacy GPS-only or GPS/GLONASS constellations, see e.g. Benoit et al. (2015), Capilla et al. (2016), Bellone et al. (2016), Yigit et al. (2016), Ferhat et al. (2017), Huntley et al. (2017), Li et al. (2017), Bouali et al. (2019). Only some exceptions can be found which tried to use also signals of new systems and a comprehensive study which would evaluate potential benefits of multi-GNSS usage in landslide

Cite this article as: Li W, Kačmařík M, Pospíšil P: Multi-GNSS positioning for landslide monitoring: a case study at the Recica landslide. Acta Geodyn. Geomater., 19, No. 3 (207), 255–270, 2022. DOI: 10.13168/AGG.2022.0011

monitoring is not available yet. Huang et al. (2017) compared GPS-only, BeiDou-only and combined GPS/BeiDou solutions of Precise Point Positioning processing (PPP; Zumberge et al., 1997; Bisnach and Gao, 2009) and showed that the positioning accuracy significantly improved for the combined constellation. Both Šegina et al. (2020) and Notti et al. (2020) tested low-cost u-blox receivers in their monitoring systems. In the first mentioned study, dual-frequency GPS/Galileo receivers were installed on a deep-seated landslide in Slovenia. In the second study, single-frequency GPS/Galileo/BeiDou receivers were utilized for an experimental continuous monitoring of an unstable slope in Italy. Lin et al. (2021) evaluated a performance of combined PPP solutions using GPS/GLONASS/BeiDou, GPS/GLONASS/Galileo and GPS/GLONASS/Galileo/BeiDou constellations at a selected landslide in China. Their results showed that all mentioned constellation combinations reached the same level of accuracy and convergence time.

Several existing GNSS positioning techniques are suitable for landslide monitoring. Differential positioning based on a combination of observations done by a receiver stabilized at the landslide and by a receiver located in the stable surroundings of the landslide is the most common. It can be implemented for a real-time monitoring using the Real Time Kinematic (RTK) technique (see i.e. Huntley et al., 2017) or in a post-processing mode as the Static relative technique (see i.e. Benoit et al., 2015; Soto et al., 2017). On the other hand, PPP technique is using un-differenced observations and therefore processing data only from a single receiver. The positioning solution can be computed on a remote device or on the receiver itself, both in real-time or post-processing mode. Its potential capabilities for landslide monitoring applications were initially discussed by Palmerini (2012). Wang (2013) applied GPS-only PPP in a monitoring of landslide in Puerto Rico. His study indicated that a horizontal accuracy below 5 mm can be stably achieved with observation data length of 4 hours and vertical accuracy below 10 mm with at least 8 hours long sessions.

Although some landslides allow a permanent installation of GNSS receivers, repetitive campaigns with temporary equipment installation are common as well. In such cases, optimal interval for campaign repetition and observation data length for a single campaign need to be addressed. In case of the observation data length, in general, the longer the session is, the higher accuracy of positioning can be expected. However, longer observation data lengths also can lead to higher costs as operators have to spend more time in the field. In such cases, it is necessary to find a suitable observation data length to reach needed level of positioning accuracy. According to Yigit et al. (2016), the minimal detectable displacement using static relative method with GPS-only constellation is about 23.4, 13.5, 9.0, 8.4 mm for 3 h, 6 h, 12 h, 24 h datasets, respectively. Alcay et al. (2019) reported a similar minimal detectable displacement in horizontal direction of 8.1 mm for 24 h datasets by using PPP technique and GPS-only constellation. In the vertical direction, the minimal detectable displacement was 19.2 mm. Gülmez and Tuşat (2017) showed that accuracy of GPS-only solutions decreased as the observation data lengths got shorter from 24 h down to 12 h, 6 h and 2 h.

Another parameter in the data collection process that deserves attention is observation sampling rate. Bahadur and Nohutcu (2020) processed data from ten MGEX stations over a one-week period, using PPP technique and 1 s, 5 s, 15 s and 30 s sampling rates. According to their results, use of high-rate (1 s) observation sampling improved the PPP performance within the first 30 minutes of solution, but the impact during longer observation lengths (exceeding 30 minutes) was small. Romero-Andrade et al. (2021) compared sampling rates from 0.1 s till 30 s for data collected by a low-cost GNSS receiver. They used PPP technique in static mode and GPS/GLONASS observations. According to their results, the low-cost GNSS receiver provided a relatively better positioning performance when the sampling rate was at 1 s and 15 s.

The main objective of this study is to analyze and evaluate positioning accuracy and performance of different satellite systems combinations with focus on finding an optimal strategy for multi-GNSS data collection and processing in landslide monitoring applications. To be more specific, following four aspects are elaborated within the study: selection of (1) constellation combination (GPS-only, GPS/Galileo, GPS/GLONASS, GPS/GLONASS/Galileo and GPS/GLONASS/Galileo/BeiDou); (2) positioning technique (PPP, differential static relative); (3) observation data length (1 h to 24 h) and (4) observation sampling rate (1 s to 30 s). The paper is organized as follows: after the introduction the study area is described, information about data collection and data processing are given. Section 3 provides results for the specified objectives based on simulating conditions of the selected landslide on data from well-established GNSS reference stations. These results are followed by an evaluation of the selected landslide deformation based on collected GNSS data. Finally, the discussion and conclusions are provided.

2. DATA AND METHODS

2.1. *STUDY AREA*

Recica landslide in the north-eastern part of the Czech Republic was selected for the study realization. It is one of the largest landslides in the Czech Republic, located on the southern slope of the side valley of the Šance reservoir built on the Ostravice river. It lies on predisposed shear surfaces (Cretaceous sandstone and claystone strata of the Silesian unit) of the outer group of Carpathians flysch zone. Geotechnical monitoring is carried out on the landslide by means of geodetic measurements,

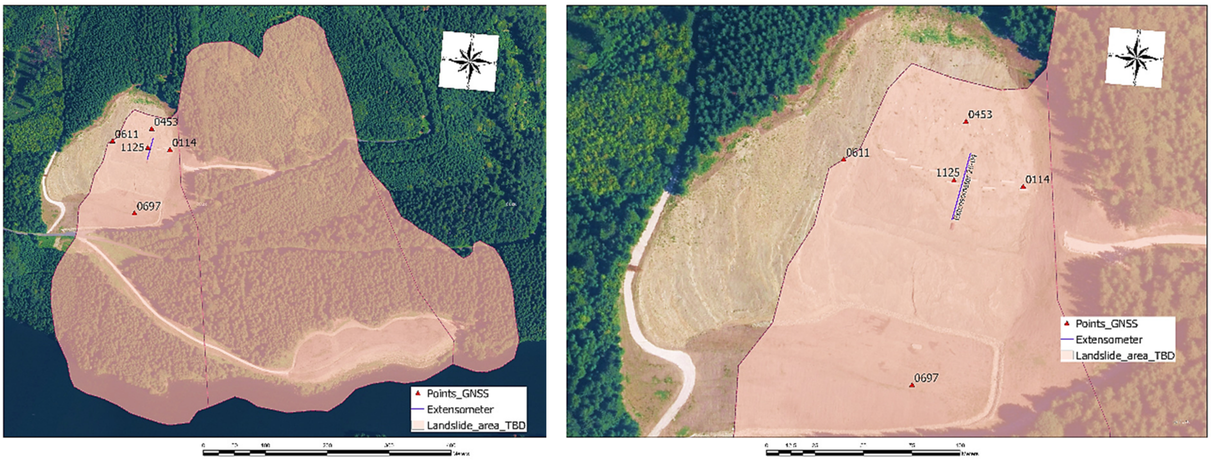

Fig. 1 Overview of the whole Recica landslide (left), position of established points for the GNSS monitoring and used extensometer (right).

inclinometric boreholes, extensometers and hydrogeological boreholes with measured groundwater levels installed at carefully selected locations so that it is possible to determine the landslide boundaries, measure the displacement of rock masses and the dynamics of movement. Corominas et al. (2000) describe application of extensometers on landslides.

Only a part of the whole landslide was recently selected for the GNSS monitoring, see Figure 1. Between years 2016 and 2018, this area was completely deforested and reclaimed in order to stabilize the landslide and take aggregates for the nearby dam reconstruction. Considering a reasonable but still partly limited sky view of the selected area, the multi-GNSS positioning can potentially bring a benefit for GNSS monitoring over the standard GPS-only or GPS+GLONASS one.

Prior to the change in terrain morphology, warning states of rock mass displacement were also established at each measurement site based on long-term observations and measurements. These were correlated with rainfall and groundwater levels, as water is probably the most important factor in initiating rock mass movement in the landslide. Following the change in terrain morphology, the rock mass behavior also changed in the western part of the landslide. It is necessary to re-learn the behavior of the rock mass forming the landslide body based on new measurements (longer data series) and to use these data as inputs to a numerical model simulating slope stability in different scenarios.

2.2. ESTABLISHMENT OF MONITORING POINTS, DATA COLLECTION

Distribution of GNSS monitoring points at landslide should generally aim on capturing its overall deformation characteristics. At the selected part of the Recica landslide, five monitoring points were stabilized using forced centering (Fig. 2) in autumn 2019 to allow a long-term GNSS monitoring based on repetitive observation campaigns.

To ensure a reasonable GNSS data collection for the presented study, twelve campaigns with a minimal duration of nine and half hours were realized between November, 2019 and October, 2021. Dates of realized campaigns are provided in Table 1. Trimble R10 receivers collecting GREC signals were used for all points except the 1125 one. During three campaigns, a smaller number of observations was collected at point 1125 with the Topcon Hiper GD receiver.

Table 1 Length of individual observation campaigns realized at the Recica landslide from November, 2019 till October, 2021.

Date	Length of observation data collection (hours)
2019-11-25	10.2
2020-04-23	10.5 (only 10.1 at point 1125)
2020-06-04	10.0
2020-07-09	10.0
2020-08-13	10.1
2020-09-18	10.0
2020-12-08	9.0 (only 6.5 at point 1125)
2021-05-31	9.6 (only 3.4 at point 1125)
2021-06-25	10.0
2021-08-06	8.9 (only 2.2 at point 1125)
2021-09-02	9.5
2021-10-08	9.6

Sky plots based on observations realized at all five monitoring points on April 23, 2020 are shown in Figure 3. Monitoring points 0114 and 0611 are located close to the boundary of the deforested area and their observation conditions are worse compared to the rest of monitoring points. These points were therefore selected for the main assessment presented within this study.

2.3. SIMULATION OF THE MONITORING POINTS LOCATED AT THE RECICA LANDSLIDE

In order to objectively evaluate potential benefits of multi-GNSS solutions over the standard GPS-only

Fig. 2 GNSS receiver Trimble R10 (left) and TOPCON Hiper GD (right) stabilized at established monitoring points.

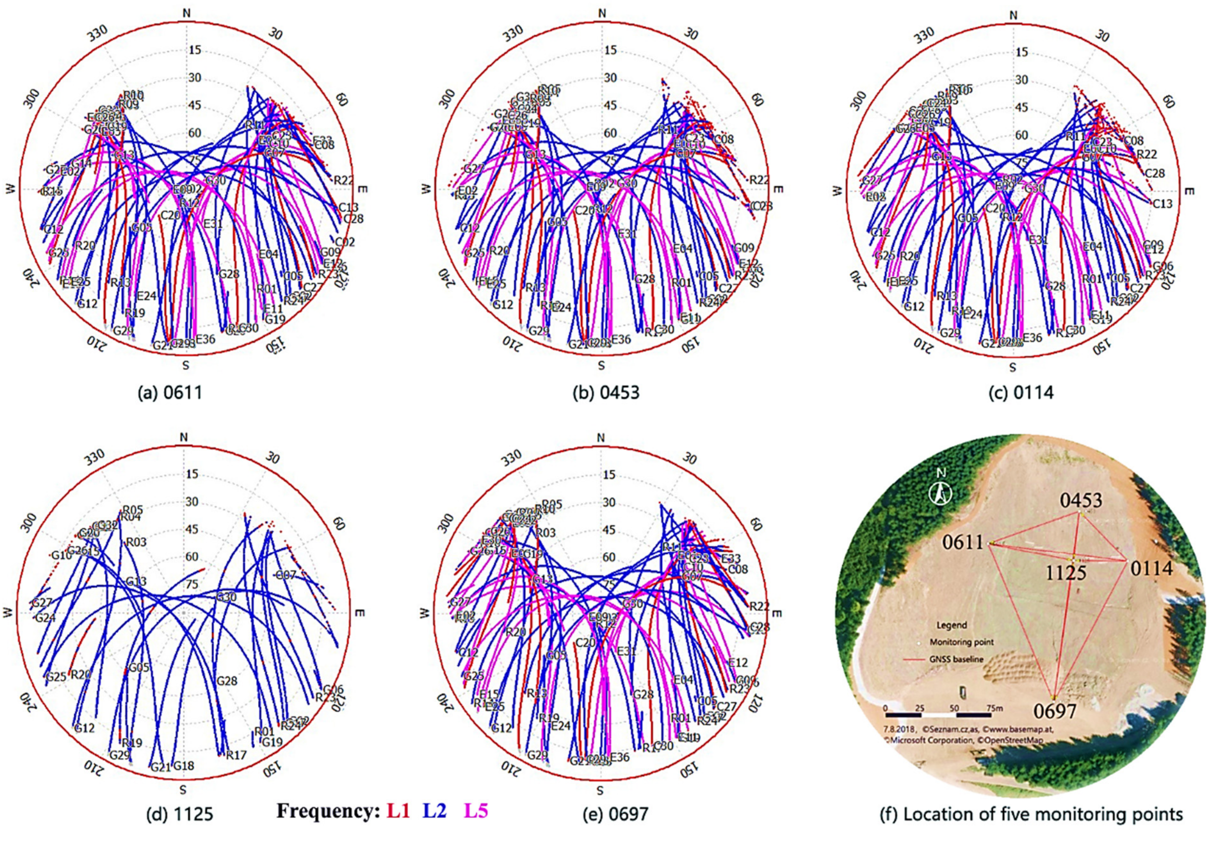

Fig. 3 Sky plots of the five monitoring points located at the Recica landslide from data collected on April 23, 2020.

or GPS/GLONASS ones and to find an optimal setting of the GNSS data collection for the Recica landslide (campaign data length, observation sampling interval), we decided to simulate observation conditions of the 0114 and 0611 points at selected well-established permanent GNSS reference stations with known precise coordinates. CPAR, CTAB and GOPE stations equipped with multi-GNSS hardware were chosen. All three are located in the Czech Republic at similar latitude as the Recica landslide, therefore receiving GNSS signals with similar geometry as points at the Recica landslide. The selected stations belong to the European Geodetic Reference Systems (EUREF) Permanent GNSS Network (EPN, https://www.epncb.oma.be/) network and are classified as class-A stations there. The distance between GOPE and CTAB (CPAR) is about 56 km (73 km), respectively.

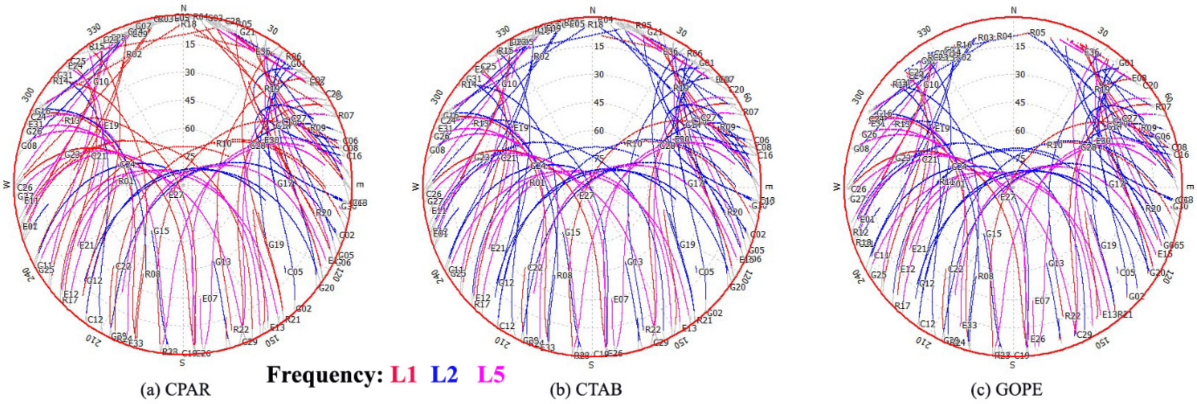

Fig. 4 Sky plots of the EUREF permanent GNSS stations selected to simulate observation conditions at the Recica landslide. From left to the right: station CPAR, CTAB and GOPE.

Observation data from these three stations were downloaded and processed (see Section 2.4) for a period of June, 2021. Two versions of processing were realized: in the first one, all available observations were used. For the second type of processing, sky view conditions of the Recica monitoring points 0114 and 0611 were simulated by applying azimuth-elevation masks and removing observations which would not be accessible on these points (see Figs. 3 and 4). An own developed tool written in Python language was used for this observation data filtering. In fact, due to limited view on the sky, about 19.2 %, 19.0 % and 18.9 % of original observations were filtered out while simulating point 0114 for CPAR, CTAB and GOPE station, respectively. Likewise, for the simulation of point 0611, these percentages were 19.8 %, 19.2 % and 19.4 %.

Station coordinates from both versions of the realized processing were later compared with coordinates from the official EPN weekly combined product (http://www.epncb.oma.be/_productsservices/analysiscentres/combinedeurefsolution.php) to assess their quality. Three statistical parameters were computed. $Mean_{3D}$ represents a mean difference between own positioning and the official EPN product in 3D dimension, computed as follows:

$$3D\_difference_i = \sqrt{\Delta x_i{}^2 + \Delta y_i{}^2 + \Delta z_i{}^2} \qquad (1)$$

$$Mean_{3D} = \frac{1}{n}\sum_i^n \mathrm{3D\_difference_i} \qquad (2)$$

x_i, Δy_i and Δz_i represent differences in the x, y, z coordinate component on the ith day.

Standard Deviation (STD) of position differences in 3D were calculated as:

$$STD_{3D} = \sqrt{\frac{1}{n}\sum_{i=1}^n[(\Delta x_i - \bar{x})^2 + (\Delta y_i - \bar{y})^2 + (\Delta z_i - \bar{z})^2]^2} \qquad (3)$$

Root Mean Square (RMS) of position differences in 3D were computed using:

$$RMS_{3D} = \sqrt{\frac{1}{n}\sum_{i=1}^n(3D\_difference_i)^2} \qquad (4)$$

2.4. GNSS DATA PROCESSING

RTKLIB software in version 2.4.3 b34 was used for GNSS data processing within this study. It is an open source program package developed for multi-GNSS navigation and positioning (Takasu, 2009; http://www.rtklib.com/). Data were processed with two different positioning techniques in static mode: 1) Precise Point Positioning technique based on un-differenced observations (abbreviated as PPP in this study); 2) differential relative technique based on double-differenced observations (abbreviated as Static relative in this study). For both techniques, extended Kalman filter running in forward mode was used to estimate unknown parameters epoch-wisely. Processed PPP solutions were based on float ambiguities while the modified least-squares ambiguity decorrelation (MLAMBDA) method (Chang et al., 2005) was applied for integer ambiguity resolution in differential solutions. Ambiguity resolution for BeiDou signals is not supported in the used version of RTKLIB.

Apart from using two different positioning techniques, data were processed with various combinations of GNSS constellations (G, GE, GR, GRE and GREC), various observation sampling rates (1 s, 5 s, 10 s, 15 s, 30 s) and various observation data lengths (1 h, 2 h, 4 h, 8 h, 10 h, 16 h, 24 h).

Basic information about applied processing strategy are given in Table 2. For more information, the reader is referred to official RTKLIB documentation (Takasu, 2009). The quality of precise orbit and clock products (below referred as precise products) has an impact on the performance of positioning, mainly for the PPP technique (see Zhou et al., 2020). Based on the assessment of multi-GNSS precise products from several analysis centers presented in Li and Kačmařík (2021), the final product

Table 2 Applied processing strategy for PPP and Static techniques.

Precise products	Final multi-GNSS product from CODE (Prange et al., 2020)
Frequency	GPS L1, L2; GLONASS L1, L2; Galileo E1, E5; BeiDou dual frequency (manual of RTKLIB does not provide information on which BeiDou frequencies are used to form a ionosphere-free linear combination)
Ionosphere	ionosphere-free linear combination
Troposphere	a priori Zenith Hydrostatic Delay (ZHD) Saastamoinen model (Saastamoinen, 1972), Zenith Total Delay (ZTD) corrections and tropospheric gradients estimated epoch-wisely
Antenna model	IGS14
Ocean tidal loading	applied (FES2004 model) (Lyard et al., 2006)
Differential code biases (DCB) files	CODE DCB monthly product
Observation sampling rate	1 s, 5 s, 10 s, 15 s, 30 s
Observation weighting	1/sin(elevation)
Elevation cut-off angle	5°
Observation data length	1 h, 2 h, 4 h, 8 h, 10 h, 16 h, 24 h
Constellation combination	G(GPS), GE(GPS/GAL), GR(GPS/GLO), GRE(GPS/GLO/GAL), GREC(GPS/GLO/GAL/BDS)

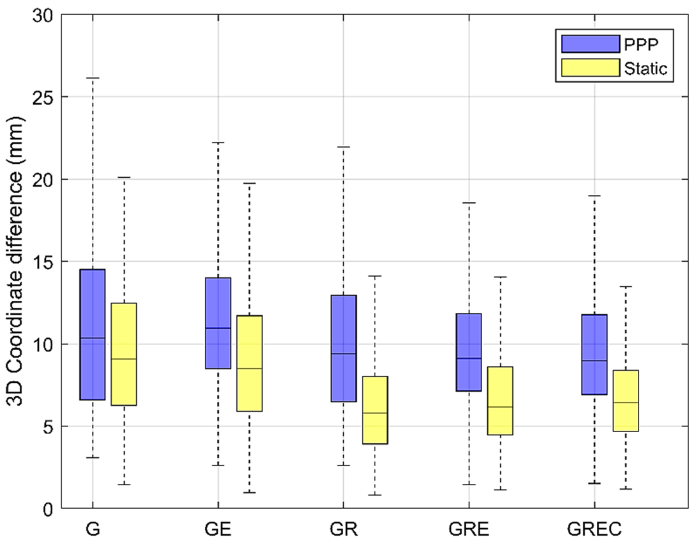

Fig. 5 Boxplot created from differences in 3D position between own processing and the official EPN weekly product. Overall results for all processed stations (CTAB, CPAR, GOPE), values for individual constellation combinations are shown from the left to the right. 24 h observation data length, 30 s sampling rate.

provided by Center for Orbit Determination in Europe (CODE, Prange et al., 2020) was selected for this study. It contains satellite ephemerides with 5 minutes' interval and satellite clock corrections with 30 second interval. No multipath analysis for observations obtained at used GNSS reference stations or at the landslide monitoring points was realized.

Bug No. 152 (http://www.rtklib.com/rtklib_support.htm) of used version of the RTKLIB software was corrected before the data processing. It was causing issues with reading SP3 files containing ephemerides data for more than 99 satellites.

3. RESULTS

Results based on simulating observation conditions of monitoring points at the Recica landslide are firstly presented and assessed. Later, an evaluation of landslide movement derived from the realized GNSS observation campaigns is provided.

3.1. *EVALUATION BASED ON SIMULATING CONDITIONS OF THE RECICA LANDSLIDE ON DATA FROM PERMANENT REFERENCE STATIONS*

3.1.1. *EVALUATION OF POSITIONING TECHNIQUE, GNSS CONSTELLATION COMBINATIONS*

As abovementioned, in order to assess a performance of various versions of GNSS positioning, we statistically compared coordinates from own processing and from the official EPN weekly product. Figure 5 shows boxplots for PPP and Static technique for various constellation

Fig. 6 Values of the 3D Mean, 3D STD and 3D RMS computed between own coordinates and the EPN weekly product. Left column shows outputs computed from all original observations, center and right columns show outputs computed from filtered observations simulating monitoring points 0114 and 0611 at the Recica landslide. Results for PPP technique (up) and Static relative positioning technique (bottom). In each sub-figure, results for individual constellation combinations are shown from left to the right. 24 h observation data length with 30 s sampling rate were used. Abbreviation as CTAB+GOPE means that CTAB was used as Rover, GOPE as Base. All values are in mm.

combinations computed over all processed stations. Coordinates from processing based on original observations as well as on filtered observations simulating monitoring points at the Recica landslide were entering this evaluation. Static relative technique reached lower median values as well as lower inter-quartile ranges, indicating a better performance compared to the PPP technique. This situation is mostly visible for GR, GRE and GREC constellation combinations.

In Figure 6, statistical parameters described in Section 2.3 are presented for Static relative and PPP technique, individually for processed stations/baselines. Almost all constellation combinations stayed below 5 mm in STD and 13 mm in RMS for Static relative technique. For the PPP, they were typically below 6 mm in STD and 15 mm in RMS. Higher quality of Static relative positioning compared to the PPP positioning was reported also by Yigit et al. (2016) or Romero-Andrade et al. (2021).

While comparing positioning results delivered by the original observations and by the filtered observations simulating Recica points, performance of the later was actually slightly better in case of the PPP technique. In case of the Static relative technique, the results were dependent on used baseline. For a baseline composed from CTAB and GOPE stations, differences between processing original observations or the filtered observations were minimal, without any evident benefit for one of the processing versions. The situation was different for a baseline given by CPAR and GOPE stations, where filtering of observations almost always led to an increase of RMS, typically between 1 to 4 mm.

From the perspective of selected constellation combination, in the Static relative positioning the best results were mostly provided by GR processing, tightly followed by GRE and GREC combinations. Utilizing GPS-only processing led to an increase of RMS between 20 % and 50 % compared to the GR combination. Combination of GE signals was slightly better than GPS-only in this regard. In the PPP positioning, when processing all station observations, GRE and GREC always provided about 1-2 mm lower RMS values than GR combination. When only the filtered observations were entering the 24 h PPP solution, results were more station dependable and performance of GR, GRE and GREC very similar. In this regard, it is necessary to note, that not all available modern BeiDou-3 satellites were processed in our study. RINEX 3 files from stations CPAR and CTAB contained only BeiDou-3 satellites with PRN code below 30 and the older BeiDou-2 satellites. Better performance of BeiDou-3 satellites compared to the

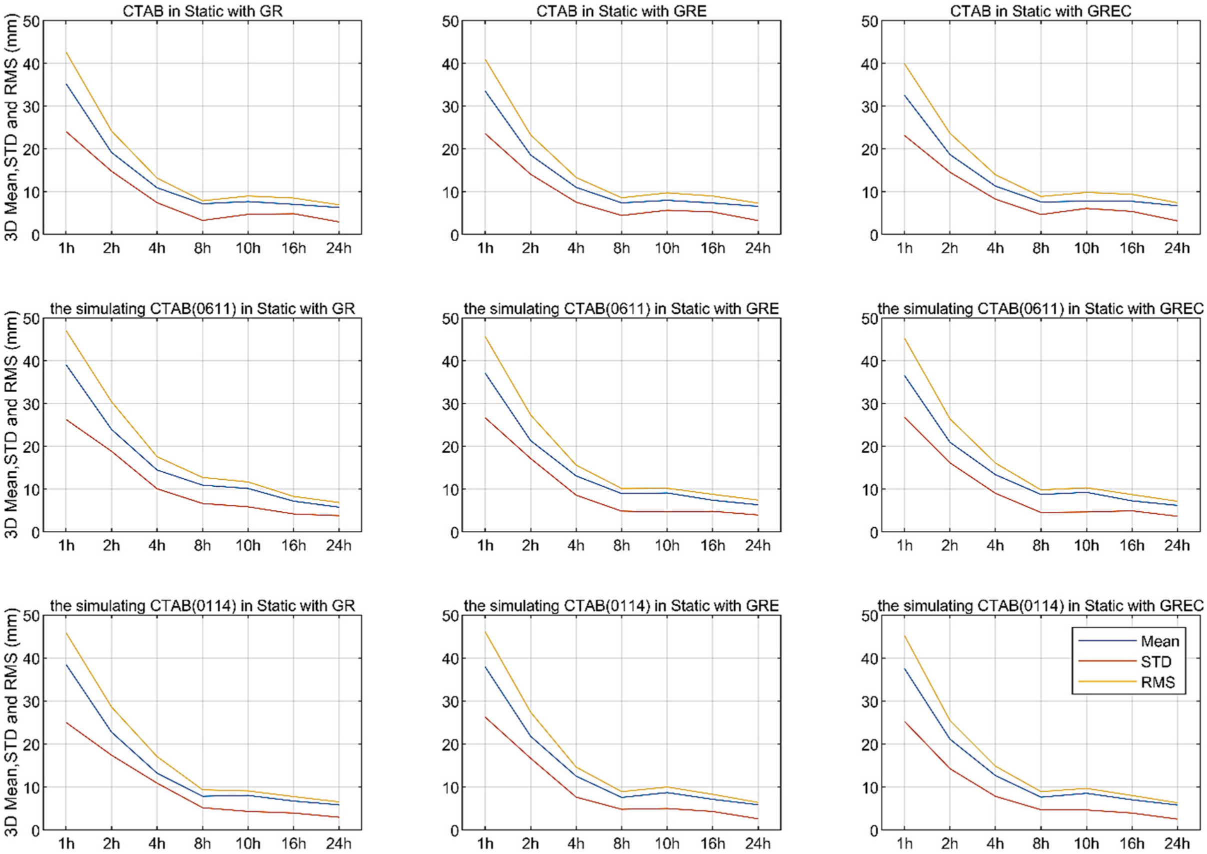

Fig. 7 3D mean, STD and RMS for various observation data lengths and constellation combinations (GR, GRE, GREC) at station CTAB. Processing was realized with Static relative technique, GOPE station was used as a BASE, 30 s observation sampling rate. All values are in mm.

BeiDou-2 ones was mentioned e.g. in Cao et al. (2021). This situation could partly influence the results achieved in our evaluation.

When using the Static relative technique, differences between results of individual baselines (CTAB+GOPE, GOPE+CTAB, or, GOPE+CPAR, CPAR+GOPE) were minimal. The baseline CTAB+GOPE was therefore selected for the assessment presented in following sub-sections 3.1.2 and 3.1.3.

3.1.2. *EVALUATION OF OBSERVATION DATA LENGTH*

In order to evaluate an impact of observation data length on positioning performance, daily (24 h) RINEX observation files with 30 s sampling rate were split into 1 h, 2 h, 4 h, 8 h, 10 h, 16 h, 24 h blocks of non-overlapping sessions. All these variants were processed for CTAB station using G, GR, GRE and GREC constellation combinations. Original observations as well as only those simulating landslide monitoring points 0114 and 0611 were processed.

In case of the Static relative technique, 8 hours long sessions reached similar results as the longer ones (see Fig. 7), with only minor improvements achieved by longer sessions. On the other hand, sessions with a duration between 1 h and 4 h all led to worse results with a clear penalty coming from shortening the observation period. The described behavior is valid for processing original observations as well as only the filtered ones. RMS values of 8 h sessions for GR, GRE and GREC constellation combinations were 7.9 mm, 8.8 mm and 8.9 mm, while STD values 3.3 mm, 4.4 mm and 4.7 mm, respectively. Performance of the GR combination was therefore better than of combinations adding Galileo or BeiDou signals to it.

In Figure 8, RMS values achieved by Static relative technique and PPP technique are given for individual observation data lengths. It can be seen that both techniques reached relatively similar performance for observation data lengths between 1 and 4 hours. For sessions of 8 hours or longer ones, Static relative technique delivered about 20-30 % better results than PPP. In other words, Static relative positioning based on 8 hours' observation data length reached a similar positioning accuracy as PPP positioning based on 24 hours, meaning RMS of about 5 mm in horizontal direction and 8 mm in vertical direction. According to these results, static relative positioning was able to more benefit from changing satellite geometry during longer data lengths compared to PPP.

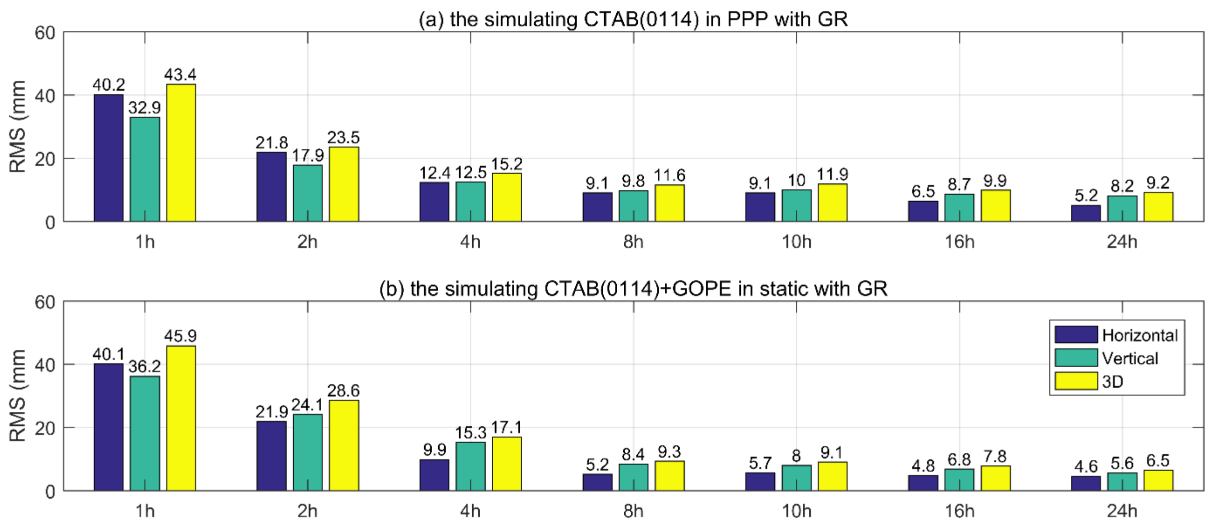

Fig. 8 RMS values (mm) in horizontal, vertical and 3D position for each observation data length.

Table 3 RMS values of comparisons based on processing data from CTAB station with various observation sampling rates (1 s, 5 s, 10 s, 15 s and 30 s). GOPE station used as Base for the Static relative technique.

Positioning techniques	Constellation combinations	Stations	Sampling rate 1 s	5 s	10 s	15 s	30 s
PPP	GR	CTAB	21.7	18	17	16.6	**14.4**
		GOPE	21.1	16.1	14.9	14.5	**14.5**
		simulating CTAB	20	16.2	15.1	14.1	**13.1**
		simulating GOPE	19.7	13.9	12.8	12.5	**12.1**
	GRE	CTAB	23	20.5	20	19.9	**18.4**
		GOPE	22.7	18.3	17.4	**17**	17.2
		simulating CTAB	22	18.7	18.1	17.9	**17.3**
		simulating GOPE	18.9	14.4	13.6	**13.6**	14.2
Static relative	GR	CTAB	17.4	12.7	11.2	10.6	**9**
		simulating CTAB	16.9	15.6	13.5	12.9	**11.7**
	GRE	CTAB	16.7	12.6	11.5	10.9	**9.7**
		simulating CTAB	15.5	13.2	13.6	13.5	**10.2**

3.1.3. *EVALUATION OF OBSERVATION SAMPLING RATE*

To evaluate an impact of various observation sampling rates on positioning performance, data from stations CTAB and GOPE were processed with PPP and Static relative techniques utilizing GR and GRE constellation combinations. Observation files spanning only over 10 hours (from 4 AM till 14 PM UTC) were downloaded and processed due to extensive size of 1s RINEX files. Using 10 h observation data lengths is also in accordance with the duration of current observation campaigns realized at the Recica landslide. Apart from using the original 1 s sampling rate, downloaded observation files were consequently filtered to 5 s, 10 s, 15 s and 30 s sampling rate.

As is visible from Table 3, performance of GNSS positioning did not improve with an increase of sampling rate. 30 s sampling rate provided almost always the best results, regardless which processing technique or constellation combination was used. Reason of this situation is most probably in the number of visible satellites and their geometry which does not improve merely by an increase of the observation sampling rate. Another reason might be related to necessity to interpolate precise products with satellite orbits and clock error corrections according to set sampling rate and their degradation because of this step.

3.2. ***RESULTS FROM THE REALIZED MONITORING CAMPAIGNS AT THE RECICA LANDSLIDE***

According to the results presented in Section 3.1, an optimal setting of GNSS data collection and processing for the Recica landslide monitoring should be as follows:

- Static relative processing technique,
- GR or GRE combination constellation,
- At least 8 h long observation data length,
- 30 s observation sampling rate.

Data collected during the twelve campaigns realized between November 2019 and October 2021 (see Section 2.2) were therefore processed in this regard, using the GR constellation combination. Multi-GNSS permanent reference station CFRM

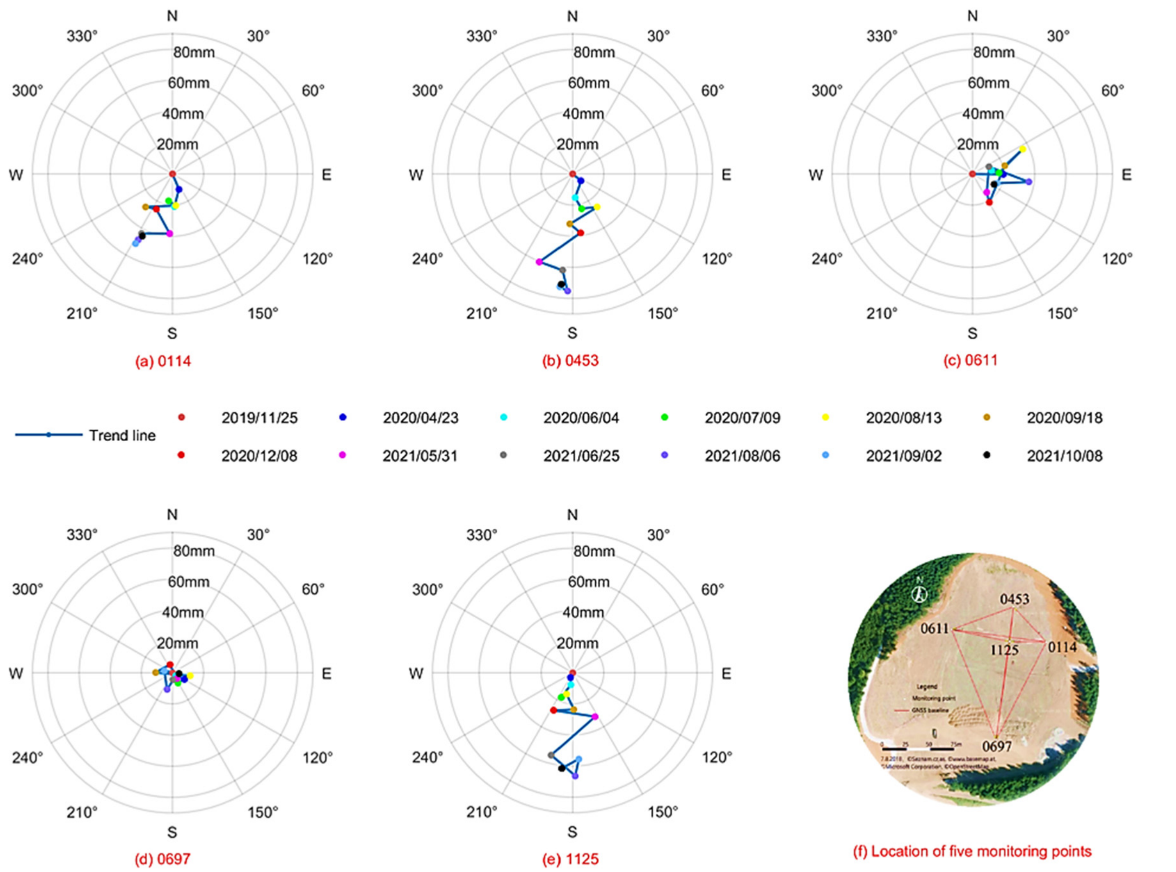

Fig. 9 Horizontal displacement of individual monitoring points at the Recica landslide over period from November 25, 2019 till October 8, 2021 shown in polar coordinate system. Static relative positioning, GR combination.

belonging to the EUREF EPN network was used as the Base station. Distance between CFRM and the Recica landslide is 20 km. CFRM coordinates from the appropriate EPN weekly combined product were entering the processing. Coordinates of monitoring points estimated for individual observation campaigns were then unified into a single reference epoch using the official ITRF velocities of the CFRM EPN reference station.

Time series showing coordinates or their changes are often used to visualize a magnitude of the landslide deformation in horizontal direction, as e.g. in Castagnetti et al. (2013) or Saleh and Becker (2019). However, with a polar coordinate system, both magnitude of deformation and movement direction can be shown simultaneously (Li et al., 2021). In Figure 9 we therefore applied this approach to present results of all five GNSS monitoring points. It can be seen that a prevailing deformation direction of monitoring points 0114, 0453 and 1125 is south, with an azimuth between 150 and 210 degrees. The largest accumulated horizontal movement of 71 mm over the studied period was found for the point 0453. Point 0611 is located on the western edge of the landslide and subjected to lateral pressure from the west, resulting in its slight eastward movement. Last point 0697 is stabilized on a flat terrain below the slope and evinced no horizontal displacement.

In terms of vertical direction, magnitude of the landslide deformation is not significantly exceeding the accuracy and precision of the GNSS positioning. Although accumulated displacements in the vertical direction presented in Figure 10 show some level of subsidence at the above described points evincing a horizontal movement, all the time series are strongly influenced by positioning errors.

Correlation between the displacements of surface points measured by GNSS and geotechnical monitoring in the area of interest is possible using data from extensometer 26-04 (Fig. 1). No other geotechnical monitoring instruments allowing a comparison with GNSS results in the area of GNSS measurements exists on the landslide. The extensometer is installed in a sub-horizontal borehole inclined 15° from the slope in the direction of fall line. The installed extensometer is Geokon 4421. It is Long Range Displacement Meter (LRDM) designed to measure up to two meters magnitude between two points. Typical applications include also monitoring of unstable slopes. The total displacement on this extensometer was 49.6 mm (Fig. 11) in two years' period between October, 2019 and September, 2021.

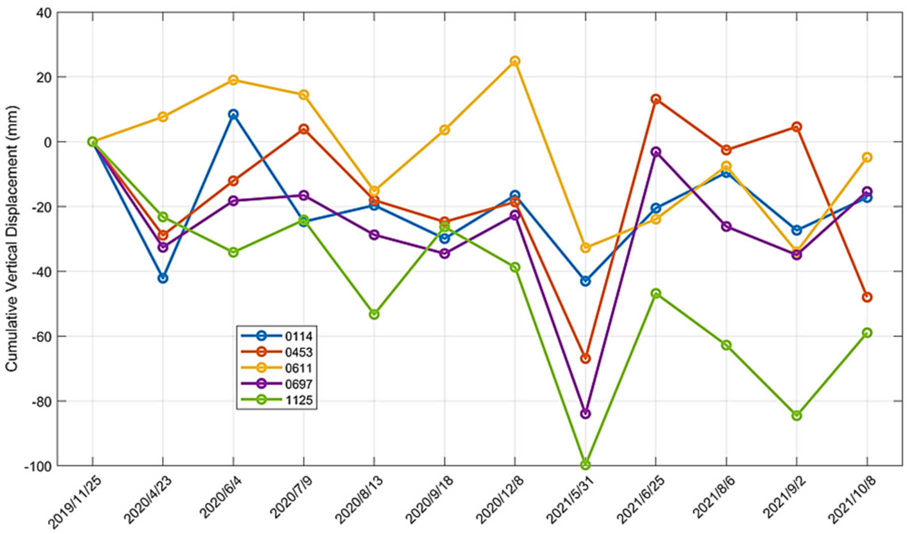

Fig. 10 Cumulative displacement in the vertical direction of monitoring points at the Recica landslide. Static relative positioning, GR combination.

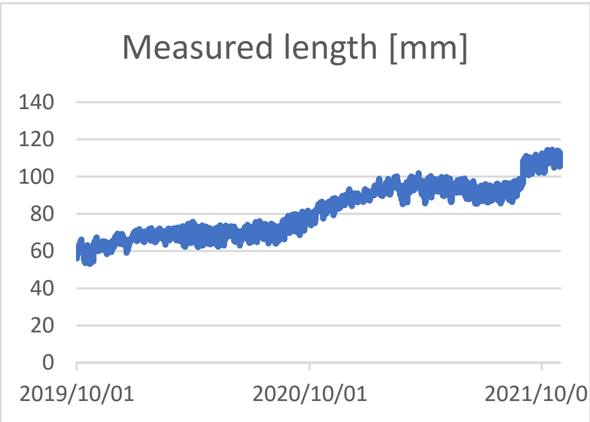

Fig. 11 Extensometer record within 2 years of measurement.

The GNSS monitoring point 1125 is the closest one to the extensometer. During the studied period which was very similar to the one used for extensometer, the horizontal displacement on this point was 61 mm.

Since application of static relative positioning does not have to be always realizable in a monitoring of selected landslide, results achieved at the Recica landslide by PPP processing are provided as well. Table 4 contains mean differences and RMS values for N, E, U coordinate components computed for GR, GRE and GREC PPP solutions. Coordinates from static relative processing based on GR combination were taken as reference. Although the results vary at individual stations and for individual coordinate components, the best agreement with the output of GR static relative positioning was found for the PPP

Table 4 Mean and RMS values for North, East and Up coordinate component comparison between PPP solutions (GR, GRE, GREC combinations) and Static relative solution (GR combination) for individual monitoring points at the Recica landslide. All values are in mm.

PPP solution	Monitoring point	North		East		Up	
		Mean	RMS	Mean	RMS	Mean	RMS
GR	0114	4	5.5	-4.4	11.4	2.3	16.6
	0453	1.6	4.2	-2.2	8.7	10.9	22.2
	0611	-0.2	5.2	-2.2	11.6	5.6	14.7
	0697	-0.5	2.8	-1.7	6.2	9	13.9
	Mean	**1.2**	**4.6**	**-2.6**	**9.8**	**7**	**17.2**
GRE	0114	-0.6	4.4	2.3	12.3	-12.9	23.7
	0453	-2.8	5.1	4.1	19.1	-6.2	22.6
	0611	-0.5	6.6	-1.9	16.3	-1.9	16.7
	0697	-4.5	6.1	2.8	9.1	-2	12.5
	Mean	**-2.1**	**5.6**	**1.8**	**14.7**	**-5.8**	**19.4**
GREC	0114	-0.2	4.3	2	12.8	-13.7	25.8
	0453	-2.9	5.4	3.1	19.8	-6.9	22.8
	0611	-0.6	6.7	-2.3	16.6	-0.7	17
	0697	-4.8	6.4	2.1	9.8	-2.2	12.8
	Mean	**-2.1**	**5.8**	**1.2**	**15.2**	**-5.9**	**20.2**

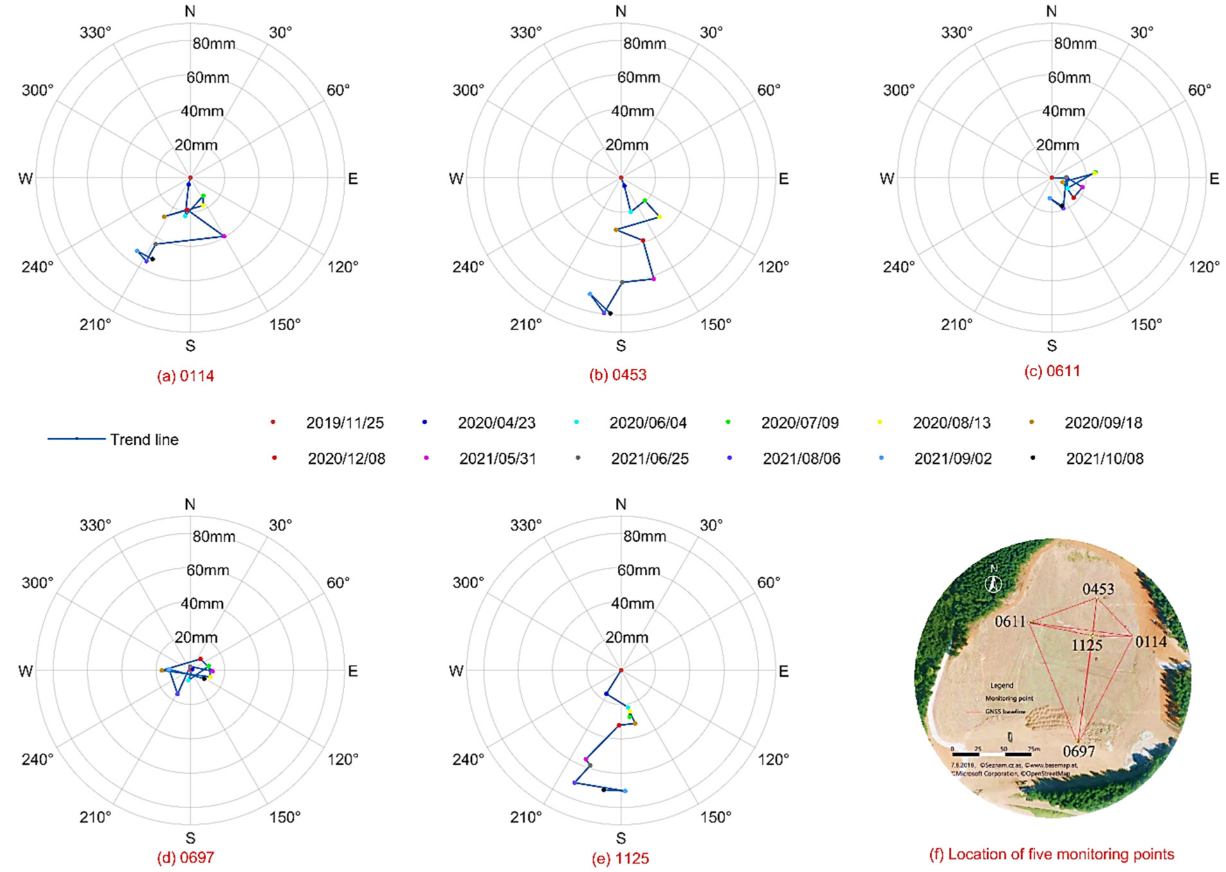

Fig. 12 Horizontal displacement of individual monitoring points at the Recica landslide over period from November 25, 2019 till October 8, 2021 shown in polar coordinate system. PPP positioning, GRE combination.

processing based on the same constellation combination. Both GRE and GREC reached higher mean RMS values at all three coordinate components. Moreover, Figure 12 plots horizontal displacement of individual monitoring points from GRE PPP processing, providing the same type of output as Figure 9. Although the output of PPP processing is visually noisier compared to the one from static relative positioning, deformation behavior of all individual points remained the same.

4. DISCUSSION

For sessions of observations lasting at least eight hours, results presented in Section 3.1 did not show any clear and ubiquitous benefit in positioning coming from processing triple or quad constellation combinations compared to the long-term established GPS+GLONASS combination. Observation geometry provided by GPS and GLONASS satellites was therefore not improved by satellites of modern systems in such an extent to increase quality of positioning. For shorter sessions lasting between one and four hours, GRE and GREC combinations typically provided about 1 to 3 mm lower RMS values compared to the GR combination. Processing all observations or only the filtered ones simulating observation conditions at the Recica landslide did not mean any difference in the described results.

Ogutcu (2020) assessed a contribution of Galileo to GPS+GLONASS PPP solutions while using observation data from 20 MGEX stations from year 2019. He found a clear positive impact of adding Galileo signals to GR in terms of convergence time. Similarly, to our study, the contribution of adding Galileo on positioning was higher as the observation data lengths become shorter. For 0.5 and 1-hour static processing, adding Galileo signals had a positive impact on RMS values at almost all processed stations. However, in case of 12 and 24-hour static processing with 5 degrees cut-off elevation angle, only 5 GNSS stations reached lower horizontal RMS values after adding Galileo signals. In terms of vertical RMS, both for 12 and 24-hour solutions, 9 GNSS stations reached higher values up to 7 mm while only about one third of GNSS stations reached lower RMS values. Moreover, Xia at el. (2019) showed that Galileo contribution to GR PPP daily static solutions was insignificant, but confirmed a positive impact on kinematic PPP solutions and on convergence time.

As already mentioned, simulating observation conditions of the Recica landslide led to deleting approximately 19 % of all accessible observations.

Still, the observations were deleted mainly from the northern parts of the sky-plot with the southern parts being practically untouched. Stations used in this study are located about 50°N in latitude where number of observations received from northern parts of the sky-plot are already partly limited due to inclination angle of GNSS satellites (see Fig. 4). Mainly observations at higher elevation angles are affected by this effect. Obstacles at the Recica landslide led therefore mostly to reducing observations at lower elevation angles which are generally of a lower quality. Based on the presented results, deterioration of the sky view at the Recica landslide seem to be not significant enough to worsen the quality of static positioning and bring any benefit of using multi-GNSS solutions when long enough data collection campaigns are used. However, the situation might be different at another locality with much worse geometry of observations as indicated by Ogutcu (2020) in his tests assessing impact of adding Galileo signals to GR combination while applying various cut-off elevation angles.

There are other aspects which might influence the described results and need to be therefore taken into consideration. First of all, Galileo system have not reached its full operational capability yet, and as was mentioned in Section 3.1, observations from all modern BeiDou-3 satellites are not always available in RINEX files provided by well-established GNSS reference stations. A significant increase of PPP positioning performance provided by a combined BeiDou-2+BeiDou3 solution compared to solely BeiDou-2 solution was reported e.g. by Jiao et al. (2019).

Development of models and processing techniques for multi-GNSS solutions as well as further improvements in quality of precise products with satellite orbits and clocks for new systems (Galileo, BeiDou) are still ongoing. In the RTKLIB software used for this study, GLONASS observations are being down-weighted by a factor of 1.5 while observations of GPS, Galileo and BeiDou systems have an identical weight of 1.0. Douša et al. (2018) used down-weighting also for observations of new systems to reflect a worse quality of their models and precise products. Kazmierski et al. (2018) tested five weighting schemes for real-time multi-GNSS processing and found out that improper or equal weighting led to decrease of coordinate repeatability.

Obtained results might be dependent also on the software used for positioning solutions. There are currently several (scientific) GNSS software with an ability to process solutions with triple or quad constellation combinations. Besides RTKLIB, Bernese GNSS software (Dach et al., 2015), GAMIT/GLOBK (http://geoweb.mit.edu/gg/), GipsyX (https://gipsy-oasis.jpl.nasa.gov) or G-Nut (Václavovic et al., 2013) can be named as common representatives. Alcay et al. (2019) realized a set of controlled displacement simulations to evaluate quality of GNSS positioning for various observation data lengths. While using Static relative technique in the GAMIT/GLOBK software with GPS only constellation, they reached RMS of 2.0 (2.8) mm in horizontal direction and 4.1 (7.9) mm in vertical direction for 24 h (8 h) observation data lengths, respectively. In our study, RMS of 4.6 (5.2) mm in horizontal direction and 5.6 (8.4) mm in vertical direction were acquired for same data lengths while processing filtered data from CTAB station with the Static relative technique and GR constellation combination. Although both studies were held under different conditions, some of the differences in positioning results might be attributable to used software for GNSS data processing and applied settings. To confirm results presented within our study mainly with respect to benefits of multi-GNSS positioning, data processing in another software could be helpful.

During last years, several authors worked on improving quality of GNSS positioning in complex environments by multipath mitigation (Su et al., 2018; Chen et al., 2019) or azimuth-dependent elevation weighting (Han et al., 2018). Some of them showed promising results while compared to standardly utilized approaches for excluding low quality observations. RTKLIB software currently offers two standard tools in this regard. Besides setting a minimum cut-off elevation angle, user can define a SNR (Signal-to-Noise Ratio) mask to exclude noisy observations. The mask can be set individually for signal frequencies and for various elevation angles. In our processing, only the first option was applied. Utilizing a more advanced approach for observation weighting or multipath mitigation could therefore lead to a further improvement in the deformation monitoring.

5. CONCLUSION

We evaluated various constellation combinations (G, GE, GR, GRE and GREC), processing techniques (PPP and Static relative), observation sampling rates (1 s, 5 s, 10 s, 15 s and 30 s) and observation data lengths (1 h, 2 h, 4 h, 8 h, 10 h, 16 h and 24 h) to study their impact on GNSS positioning used for landslide monitoring. While processing data from well-established GNSS reference stations we simulated limited sky-view of the monitoring points which were established at the existing Recica landslide in the Czech Republic.

In terms of processing technique, Static relative positioning offered about 20-30 % lower RMS values compared to PPP technique when observation data lengths of at least eight hours were used. For shorter data lengths, both techniques performed similarly. As rather long baselines of 56 km and 73 km were used in this study, their shortening could lead to a further improvement in Static relative solutions. In overall, when it is possible to use the differential technique in the landslide monitoring application, it can be recommended over the PPP.

The results shown that accuracy of positioning is increasing exponentially with prolongation of observation time within the first eight hours and further improves only slightly with longer periods. Observation data lengths of at least 8 hours should be therefore used for monitoring based on repetitive campaigns when GNSS receivers cannot be permanently installed on landslide. Increasing sampling interval of observations did not bring any improvement in positioning and standard 30 s interval can be recommended for post-processed processing with above mentioned observation data lengths.

With observation data lengths of at least eight hours, best positioning was typically reached when using a combination of legacy GPS and GLONASS systems. Adding signals from modern Galileo or BeiDou system led to positive impact only in some cases. On the other hand, a positive income of their adding was found for shorter observation data lengths. It is therefore hard to give a universal recommendation on GNSS constellation combination to be used in every case. The situation might change with a complete finalization of new systems, existence of precise models for them and improvements in processing strategies for triple and quad constellations. The results were correlated with geotechnical extensometer measurements.

REFERENCES

Alcay, S., Ogutcu, S., Kalayci, I., Ozer, C. and Yigit, Y.: 2019, Displacement monitoring performance of relative positioning and Precise Point Positioning (PPP) methods using simulation apparatus. Adv. Space Res., 63, 1697–1707. DOI: 10.1016/j.asr.2018.11.003

Bahadur, B. and Nohutcu, M.: 2020, Impact of observation sampling rate on Multi-GNSS static PPP performance. Surv. Rev., 53, 378, 206–215. DOI: 10.1080/00396265.2019.1711346

Bellone, T., Dabove, P., Manzino, A.M. and Taglioretti, C.: 2016, Real-time monitoring for fast deformations using GNSS low-cost receivers. Geomat. Nat. Hazards Risk, 7, 2, 458–470. DOI: 10.1080/19475705.2014.966867

Benoit, L., Briole, P., Martin, O., Thom, C., Malet, J.-P. and Ulrich, P.: 2015, Monitoring landslide displacements with the Geocube wireless network of low-cost GPS. Eng. Geol., 195, 111–121. DOI: 10.1016/j.enggeo.2015.05.020

Bisnath, S. and Gao, Y.: 2009, Precise point positioning a powerful technique with a promising future. GPS World, 20, 4, 43–50.

Bouali, E.H., Oommen, T. and Escobar-Wolf, R.: 2019, Evidence of instability in previously-mapped landslides as measured using GPS, optical, and SAR data between 2007 and 2017: A case study in the Portuguese bend landslide complex, California. Remote Sens., 11, 8, 937. DOI: 10.3390/rs11080937

Calcaterra, S., Cesi, C., Maio, C.D., Gambino, P., Merli, K. and Vallario, M.: 2012, Surface displacements of two landslides evaluated by GPS and inclinometer systems: a case study in Southern Apennines, Italy. Nat. Hazards, 61, 1, 257–266. DOI: 10.1007/s11069-010-9633-3

Cao, X., Shen, F., Zhang, S. and Li, J.: 2021, Satellite availability and positioning performance of uncombined precise point positioning using BeiDou-2 and BeiDou-3 multi-frequency signals. Adv. Space Res., 67, 4, 1303–1316. DOI: 10.1016/j.asr.2020.11.011

Capilla, R., Berné, J., Martín, A. and Rodrigo, R.: 2016, Simulation case study of deformations and landslides using real-time GNSS precise point positioning technique. Geomat. Nat. Hazards Risk, 7, 6, 1856–1873. DOI: 10.1080/19475705.2015.1137243

Castagnetti, C., Bertacchini, E., Corsini, A. and Capra, A.: 2013, Multi-sensors integrated system for landslide monitoring: critical issues in system setup and data management. Eur. J. Remote Sens., 46, 1, 104–124. DOI: 10.5721/EuJRS20134607

Chang, X.-W., Yang, X. and Zhou, T.: 2005, MLAMBDA: A modified LAMBDA method for integer least-squares estimation. J. Geod.79, 9, 552–565. DOI: 10.1007/s00190-005-0004-x

Corominas, J., Moya, J., Lloret, A., Gili, J.A., Angeli, M.G., Pasuto, A. and Silvano, S.: 2000, Measurement of landslide displacements using a wire extensometer. Eng. Geol., 55, 3, 149–166. DOI: 10.1016/S0013-7952(99)00086-1

Chen, C., Chang, G., Zheng, N. and Xu, T.: 2019, GNSS multipath error modeling and mitigation by using sparsity-promoting regularization. IEEE Access, 7, 24096–24108. DOI: 10.1109/ACCESS.2019.2899622

Devoti, R., Zuliani, D., Braitenberg, C., Fabris, P. and Grillo, B.: 2015, Hydrologically induced slope deformations detected by GPS and clinometric surveys in the Cansiglio Plateau, southern Alps. Earth Planet. Sci. Lett., 419, 134–142. DOI: 10.1016/j.epsl.2015.03.023

Dach, R., Lutz, S., Walser, P. and Fridez, P. (Eds): 2015, Bernese GNSS Software Version 5.2. User manual. Astronomical Institute, University of Bern, Bern. Open Publishing. DOI: 10.7892/boris.72297

Douša, J., Václavovic, Zhao, L. and Kačmařík, M.: 2018, New adaptable all-in-one strategy for estimating advanced tropospheric parameters and using real-time orbits and clocks. Remote Sens., 10, 232. DOI: 10.3390/rs10020232

Ferhat, G., Malet, J.P., Puissant, A., Caubet, D. and Hubert, E.: 2017, Geodetic monitoring of the Adroit landslide, Barcelonnette, French Southern Alps. 7th International Conference on Engineering Surveying - INGEO 2017, Lisbon, Portugal.

Gili, J.A., Corominas, J. and Rius, J.: 2000, Using Global Positioning System techniques in landslide monitoring. Eng. Geol., 55, 3, 167–192. DOI: 10.1016/S0013-7952(99)00127-1

González-Díez, A., Remondo, J., Díaz de Terán, J.R. and Cendrero, A.: 1999, A methodological approach for the analysis of the temporal occurrence and triggering factors of landslides. Geomorphology, 30, 1–2, 1999, 95–113. DOI: 10.1016/S0169-555X(99)00047-1

Gülmez, S. and Tuşat, E.: 2017, The analysis of GPS data in different observation periods using online GNSS Process Services. Int. J. Environ. Geoinformatics, 4, 1, 43–53. DOI: 10.30897/ijegeo.306492

Han, J., Huang, G., Zhang, Q., Tu, R., Du, Y. and Wang, X.: 2018, A new azimuth-dependent elevation weight (ADEW) model for real-time deformation monitoring in complex environment by Multi-GNSS. Sensors, 18, 2473. DOI: 10.3390/s18082473

Huang, G., Du, Y., Meng, L., Huang, G., Wang, J. and Han, J.: 2017, Application performance analysis of three GNSS precise positioning technology in landslide monitoring. Lect. Notes Electr. Eng., 437, 139–150. DOI: 10.1007/978-981-10-4588-2_12

Huntley, D.H., Bobrowsky, P., Parry, N., Bauman, P., Candy, C. and Best, M.: 2017, Ripley landslide: the geophysical properties of a slow-moving landslide near Ashcroft, British Columbia. Natural Resources Canada, Geological Survey of Canada. Open File 8062, 66 pp. DOI: 10.4095/300563

Jiao, G., Song, S., Ge, Y., Su, K. and Liu, Y.: 2019, Assessment of BeiDou-3 and Multi-GNSS Precise Point Positioning Performance. Sensors, 19, 2496. DOI: 10.3390/s19112496

Kazmierski, K., Hadas, T. and Sosnica, K.: 2018, Weighting of Multi-GNSS observations in real-time precise point positioning. Remote Sens., 10, 84. DOI: 10.3390/rs10010084

Li, X., Zhang, X., Ren, X. et al.: 2015, Precise positioning with current multi-constellation Global Navigation Satellite Systems: GPS, GLONASS, Galileo and BeiDou. Sci. Rep., 5, 8328. DOI: 10.1038/srep08328

Li, Y., Huang, J., Jiang, S., Huang, F. and Chang, Z.: 2017, A web-based GNSS system for displacement monitoring and failure mechanism analysis of reservoir landslide. Sci. Rep., 7, 17171. DOI: 10.1038/s41598-017-17507-7

Li, P., Jiang, X., Zhang, X., Ge, M. and Schuh, H.: 2020, GPS + Galileo + BeiDou precise point positioning with triple-frequency ambiguity resolution. GPS Solut., 24, 78. DOI: 10.1007/s10291-020-00992-1

Li, W. and Kačmařík, M.: 2021, Assessment of multi-GNSS precise orbit and clock products from different analysis centers based on precise point positioning. Acta Geodyn. Geomater., 18, 3(203), 387–397. DOI: 10.13168/AGG.2021.0027

Li, W., Igor, I., Liu, Y. and Yang, L.: 2021, Visual processing and analysis of landslide deformation based on GNSS. IEEE Sens. J., 21, 22, 25260–25266. DOI: 10.1109/JSEN.2021.3061256

Li, M., Xu, T., Guan, M. et al.: 2022, LEO-constellation-augmented multi-GNSS real-time PPP for rapid re-convergence in harsh environments. GPS Solut., 26, 1. DOI: 10.1007/s10291-021-01217-9

Lin, C., Wu, G., Feng, X., Li, D., Yu, Z., Wang, X., Gao, Y., Guo, J., Wen, X. and Jian, W.: 2021, Application of multi-system combination precise point positioning in landslide monitoring. Appl. Sci., 11, 18, 8378. DOI: 10.3390/app11188378

Lyard, F., Lefevre, F., Letellier, T. and Francis, O.: 2006, Modelling the global ocean tides: modern insights from FES2004. Ocean Dyn., 56, 5-6, 394–415. DOI: 10.1007/s10236-006-0086-x

Malet, J.-P., Maquaire, O. and Calais, E.: 2002, The use of Global Positioning System techniques for the continuous monitoring of landslides: application to the Super-Sauze earthflow (Alpes-de-Haute-Provence, France). Geomorphology, 43, 1-2, 33–54. DOI: 10.1016/S0169-555X(01)00098-8

Montenbruck, O., Steigenberger, P., Prange, L., Deng, Z., Zhao, Q., Perosanz, F. et al.: 2017, The Multi-GNSS experiment (MGEX) of the international GNSS service (IGS)–achievements, prospects and challenges. Adv. Space Res., 59, 7, 1671–1697. DOI: 10.1016/j.asr.2017.01.011

Notti, D., Cina, A., Manzino, A., Colombo, A., Bendea, I.H., Mollo, P. and Giordan, D.: 2020, Low-Cost GNSS solution for continuous monitoring of slope instabilities applied to Madonna Del Sasso Sanctuary (NW Italy). Sensors, 20, 289. DOI: 10.3390/s20010289

Ogutcu, S.: 2020, Assessing the contribution of Galileo to GPS+GLONASS PPP: Towards full operational capability. Measurement, 151. DOI: 10.1016/j.measurement.2019.107143

Palmerini, G.: 2012, Capabilities of the GNSS Precise Point Positioning technique for landslide monitoring. Disaster Adv., 5, 4, 509–513.

Pan, Z., Chai, H. and Kong, Y.: 2017, Integrating multi-GNSS to improve the performance of precise point positioning. Adv. Space Res., 60, 2596–2606. DOI: 10.1016/j.asr.2017.01.014

Pan, L., Zhang, X., Li, X., Li, X., Lu, C., Liu, J. and Wang, Q.: 2019, Satellite availability and point positioning accuracy evaluation on a global scale for integration of GPS, GLONASS, BeiDou and Galileo. Adv. Space Res., 63, 2696–2710. DOI: 10.1016/j.asr.2017.07.029

Paziewski, J., Fortunato, M., Mazzoni, A. and Odolinski, R.: 2021, An analysis of multi-GNSS observations tracked by recent Android smartphones and smartphone-only relative positioning results. Measurement, 175, 109162. DOI: 10.1016/j.measurement.2021.109162

Pecoraro, G., Calvello, M. and Piciullo, L.: 2019, Monitoring strategies for local landslide early warning systems. Landslides, 16, 2, 213–231. DOI: 10.1007/s10346-018-1068-z

Prange, L., Arnold, D., Dach, R., Kalarus, M., Schaer, S., Stebler, P., Villiger, A. and Jäggi, A.: 2020, CODE product series for the IGS MGEX project. Astronomical Institute, University of Bern. DOI: 10.7892/boris.75882.3

Romero-Andrade, R., Trejo-Soto, M.E., Vázquez-Ontiveros, J.R., Hernández-Andrade, D. and Cabanillas-Zavala, J.L.: 2021, Sampling rate impact on precise point positioning with a low-cost GNSS receiver. Appl. Sci., 11, 16, 7669. DOI: 10.3390/app11167669

Saastamoinen, J.: 1972, Contributions to the theory of atmospheric refraction. Bull. Geod, 105. 1, 279–298. DOI: 10.1007/BF02521844

Saleh, M. and Becker, M.: 2019, New estimation of Nile Delta subsidence rates from InSAR and GPS analysis. Environ. Earth Sci., 78, 6. DOI: 10.1007/s12665-018-8001-6

Soto, J., Galve, J.P., Palenzuela, A.A., Azañón, J.M., Tamay, J. and Irigaray, C.: 2017, A multi-method approach for the characterization of landslides in an intramontane basin in the Andes (Loja, Ecuador). Landslides, 14, 1929–1947. DOI: 10.1007/s10346-017-0830-y

Šegina, E., Peternel, T., Urbančič, T., Realini, E., Zupan, M., Jež, J., Caldera, S., Gatti, A., Tagliaferro, G., Consoli, A., González, J.R. and Auflič, M.J.: 2020, Monitoring surface displacement of a deep-seated landslide by a low-cost and near real-time GNSS system. Remote Sens., 12, 20, 1–26. DOI: 10.3390/rs12203375

Su, Lj., Hu, Kh. and Zhang, Wf.: 2017, Characteristics and triggering mechanism of Xinmo landslide on 24 June 2017 in Sichuan, China. J. Mt. Sci., 14, 1689–1700. DOI: 10.1007/s11629-017-4609-3

Su, M., Zheng, J., Yang, Y. and Wu, Q.: 2018, A new multipath mitigation method based on adaptive thresholding wavelet denoising and double reference shift strategy. GPS Solut., 22, 2. DOI: 10.1007/s10291-018-0708-z

Takasu, T.: 2009, RTKLIB: Open Source Program Package for RTK-GPS. Proc. FOSS4G 2009, Tokyo, Japan, November 2, 2009.

Václavovic, P., Douša, J. and Gyori, G.: 2013, G-Nut software library – state of development and first results. Acta Geodyn. Geomater., 10, 4(172), 431–436. DOI: 10.13168/AGG.2013.0042

Vega, J.A., Marín, N. and Hidalgo, C.: 2019, Statistical approaches for the assessment of landslide related economic losses. IOP Conf. Series: Materials Science and Engineering, 471, 102009. DOI: 10.1088/1757-899X/471/10/102009

Wang, G.: 2013, Millimeter-accuracy GPS landslide monitoring using precise point positioning with single receiver phase ambiguity (PPPSRPA) resolution: A case study in Puerto Rico. J. Geodetic Sci., 3, 1, 22–31. DOI: 10.2478/jogs-2013-0001

Xia, F., Ye, S., Xia, P., Zhao, L., Jiang, N., Chen, D. and Hu, G.: 2019, Assessing the latest performance of Galileo-only PPP and the contribution of Galileo to Multi-GNSS PPP. Adv. Space Res., 63, 2784–2795. DOI: 10.1016/j.asr.2018.06.008

Yigit, C.O., Coskun, M., Yavasoglu, H., Arslan, A. and Kalkan, Y.: 2016, The potential of GPS Precise Point Positioning method for point displacement monitoring: A case study. Measurement, 91, 398–404. DOI: 10.1016/j.measurement.2016.05.074

Zhou, F., Cao, X. and Ge, Y.: 2020, Assessment of the positioning performance and tropospheric delay retrieval with precise point positioning using products from different analysis centers. GPS Solut., 24, 12. DOI: 10.1007/s10291-019-0925-0

Zumberge, J.F., Heflin, M.B., Jefferson, D.C., Watkins, M.M. and Webb, F.H.: 1997, Precise point positioning for the efficient and robust analysis of GPS data from large networks. J. Geophys. Res., 102, 5005–5017. DOI: 10.1029/96JB03860